Interaction Potentials and Vibrational Effects in the Acetylene Dimer

Kimberly Shuler and Clifford E. Dykstra*

Department of Chemistry, Indiana University−Purdue University Indianapolis, 402 N. Blackford Street, Indianapolis, Indiana 46202

Received: November 15, 1999; In Final Form: February 28, 2000

Ab initio calculations were carried out for critical point regions of the acetylene dimer potential surface with different basis sets, with and without the inclusion of counterpoise correction, and at two different electron correlation levels. The results were used to determine parameters for model interaction potentials with different forms for their electrostatic terms. Vibrational quantum Monte Carlo calculations for rigid monomers were performed using each of the model potentials, and refinements of the few parameters in the model potentials were obtained, such that the calculated rotational constant for the ground vibrational state matched the experimentally determined value. Comparison of features of the resulting surfaces showed that similar surfaces could be obtained from the different ab initio starting points, an indication of the suitability of the potentials' forms and of the nature of lingering errors in the ab initio treatments. This provides a very useful basis for more general model development. Specific information obtained about the acetylene dimer is that the changes in the rotational constant due to vibrational averaging are about 2% and that the dissociation energy from the ground vibrational state is about 400 cm^{-1}.

Introduction

One reason for interest in the weak interaction of acetylene with rare gas atoms and with other molecular partners is that although acetylene has no net dipole, it has hydrogens that may participate in hydrogen bonding. Generally, the interaction strength of acetylene for partner molecules or molecular clusters is small relative to those of molecules with permanent dipoles (e.g., water), and hence, acetylene provides a special probe of the complicated juxtaposition of effects that comprise noncovalent and hydrogen bonding interactions.

The acetylene dimer has been the subject of a number of key experimental studies,[1−11] and it is known to have a T-shaped equilibrium structure, a result verified by ab initio studies.[12−18] Although the T-shaped structure is consistent with the attractive interaction of the acetylenes' quadrupoles, the interaction is more complicated in that the quadrupole−quadrupole interaction is only a share of the total interaction strength at equilibrium. In an effort to understand the contributing effects of the acetylene−acetylene interaction at a detailed level suited to deriving elements for transferable potential parameters, a series of ab initio calculations were carried out for the acetylene dimer. These were used to locate three symmetry-constrained minima and map out limited regions of the potential surface in their vicinity. The three structures test different features of a representation (e.g., model) of the interaction surface. A further assessment of the model potentials was accomplished through the calculation of ground vibrational state properties.

There have been a number of studies wherein the acetylene−acetylene interaction potential has been modeled, fitted, or otherwise represented.[18−22] In many cases, this was done in the course of performing a partial dynamical analysis, sometimes for the interesting interconversion process in the acetylene dimer and/or for vibrational energies. Our primary interest in performing new ab initio calculations on the acetylene dimer was in model potential development. Relatively simple forms for the potentials of weakly interacting species can often serve to represent key surface features, and their simplicity makes them attractive for dynamical analysis and mixed quantum mechanical−molecular mechanics approaches. More features can be represented and/or accuracy improved with increasing the complexity of the functional form of an interaction potential, and hence, one is ultimately concerned with the tradeoff between the quality of the representation and the computational cost of using it in dynamical simulations. In addition to this concern, we wish to understand, and exploit as much as possible, the transferability of potential parameters, such as the values for electrical moments and polarizabilities of the constituent monomers. These two considerations often guide the selection of potential forms used for the study of weakly bound clusters.

Theoretical Approach

Ab initio calculations were performed for $(HCCH)_2$ with the monomer bond lengths fixed at values obtained by Assfeld et al.,[23] $R_{CC} = 1.2143$ Å and $R_{CH} = 1.0649$ Å. The cc-pVTZ basis set of Dunning[24] was used in most of the calculations, and it consisted of 176 basis functions for $(HCCH)_2$. Certain test calculations were performed with this set, augmented with additional even-tempered uncontracted functions, one set of diffuse s functions on each center (exponents = 0.0324 [H] and 0.0453 [C]), one set of diffuse p functions (exponents = 0.107 [H] and 0.0382 [C]), and two sets of diffuse d functions on the carbon centers (exponents = 0.0922 and 0.0267 [C]) for a total of 248 functions. Counterpoise correction for basis set superposition error (designated herein with "/cc") was made with the Boys−Bernardi scheme.[25]

Correlation energies were evaluated at the MP2 level of treatment, with selected tests done with the double substitution coupled cluster treatment ACCD (approximate double substitution coupled cluster,[26] a treatment first developed as ACP-D45 by Jankowski and Paldus.[27] ACCD or ACP-D45 exploits a near cancellation in certain small Hamiltonian matrix elements in

10.1021/jp9940405 CCC: $19.00
Published on Web 04/26/2000

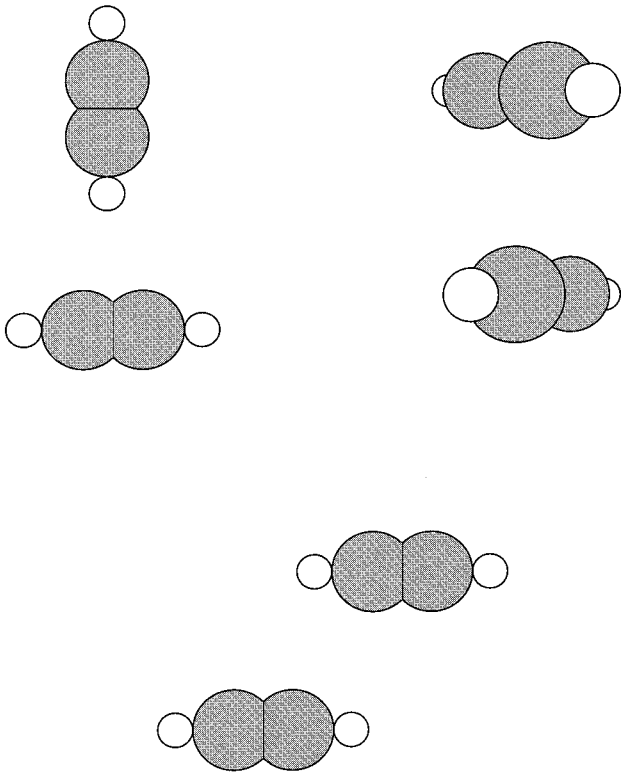

Figure 1. The three structures of the acetylene dimer characterized by ab initio calculations. The planar T-shaped structure (upper left) is the global minimum. The slipped parallel structure (bottom) is a planar structure constrained in the geometry optimization to have C_{2h} symmetry, and the crossed structure (upper right) has the monomers perpendicular, constrained to D_{2d} symmetry.

the CCD treatment and produces property values and potential surfaces very similar to CCD.[28,29]

The model potentials used to represent the dimer surface followed the molecular mechanics for clusters (MMC) scheme[30] in expressing the interaction as a sum of the classically evaluated electrical interaction energy plus Lennard−Jones or 6−12 terms among different monomer sites. The electrical interaction is the sum of the permanent moment interaction and polarization energy based on the dipole and quadrupole polarizabilities of the monomers, whereas the 6−12 terms are treated with adjustable parameters. Here, the adjustment of these parameters was done first to match the ab initio description of the surface in the vicinity of the T-shaped global equilibrium structure and the lowest energy crossed and slipped parallel structures (Figure 1). Different parameter sets were determined for different sets of ab initio data and with three representations of acetylene's permanent charge field.

Using each of the model potentials, vibrational analysis was carried out for $(HCCH)_2$ via rigid body diffusion quantum Monte Carlo (RBDQMC) calculation. This treatment follows Anderson's diffusion quantum Monte Carlo (DQMC) approach[31] but with the complication that the diffusion steps must include the rotation of the rigid molecule about its principal axes in addition to the translation of the mass centers. The advantage is that for a given precision in the simulation, longer time steps can be used because the high frequency intramolecular vibrational motions are excluded via the imposition of monomer rigidity. A number of RBDQMC calculations have been reported for weakly bound clusters,[32−39] and in particular, Gregory and Clary have shown good agreement of DQMC and RBDQMC for zero-point energies and rotational constants.[35] For the RBDQMC calculational results given here, the time step was 4.0 au (time) [1.0 au (time) or 1.0 h/($2\pi E_h$) = 2.418 88 × 10^{-17} s]. The number of QMC-psips was 8000, and the energy and property evaluations were performed through 126 000 time steps each. These were carried out following an equilibration sequence of at least 10 000 time steps of decreasing size and an overall duration of 6 × 10^5 au.

TABLE 1: Comparison of $(HCCH)_2$ Energies at a near Equilibrium Structure[a]

level of treatment[b]	electronic energy (au)	interaction energy (cm^{-1})
	176-function basis	
SCF	−153.696 72	184
SCF/cc	−153.696 59	157
MP2	−154.379 86	622
MP2 (SCF/cc)	−154.379 74	595
MP2/cc	−154.379 24	487
ACCD	−154.392 85	518
ACCD (SCF/cc)	−154.392 73	491
ACCD/cc	−154.392 27	391
	248-function basis	
SCF	−153.697 66	160
SCF/cc	−153.697 59	146
MP2	−154.385 20	687
MP2 (SCF/cc)	−154.385 13	673
MP2/cc	−154.384 43	519

[a] T-shaped structure with R_{com} = 4.3246 Å. [b] "/cc" designates counterpoise correction.[25]

The RBDQMC simulation yielded weights that reflect, but are not strictly, those of the vibrational state probability densities.[40] The true probability density may be obtained by descendant weighting,[41,42] and thus, rotational constants were calculated by averaging the inverses of the principal moments of inertia with these probability densities. More direct connection with spectroscopic measurement is obtainable from calculations that yield rotational excited-state energies and sets of transition energies such that rotational constants can be obtained following the same analysis applied to spectroscopic data.[43,44] We expect the errors from the averaging approach to be small and comparable to other lingering error sources, such as the assumed rigidity of HCCH. Finally, a readjustment of parameters in the model potentials was performed to bring the RBDQMC values of the rotational constants in line with spectroscopic values. The changes in the surfaces from this refinement serve to characterize the lingering errors in the ab initio information and the suitability of the form of the model potential in ways discussed below.

Results and Discussion

Ab Initio Calculations. For the different levels of calculation that were performed, Table 1 gives the calculated electronic energies of a near equilibrium (T-shaped) structure, one of the surface points evaluated at all levels. Also given are the interaction energies, which are expressed here as energies at a given structure subtracted from the corresponding energies of two noninteracting monomers. Positive values correspond to attractive interaction.

The values in Table 1 reveal first that the counterpoise correction with the cc-pVTZ (176 function) basis at the SCF level is small, 27 cm^{-1}. Of course, SCF is insufficient to decsribe the interaction fully, and correlation effects deepen the well in this region by at least 300 cm^{-1}. The MP2 interaction energy for the specific T-shaped structure of Table 1 is 622 cm^{-1}. The counterpoise correction to the correlation energy of 108 cm^{-1} is also more than the corresponding SCF correction. The enlargement of the basis with diffuse functions (248-function set) reduces the interaction energy at the SCF level by 24 cm^{-1}.

TABLE 2: Minimum Energy T-Shaped Structures of $(HCCH)_2$ from ab Initio Calculations

	R_{com} (Å)	$(B_{eq}+C_{eq})/2$ (MHz)	interaction energy D_e (cm^{-1})
	176-function basis		
MP2	4.285	1941	595
MP2 (SCF/cc)	4.293	1934	596
MP2/cc	4.381	1863	490
ACCD/cc	4.472	1794	410
	248-function basis		
MP2	4.285	1941	677
MP2 (SCF/cc)	4.303	1927	678
MP2/cc	4.358	1882	530

Mostly, this corresponds to diminishing the lingering basis set superposition error, and consequently, the SCF interaction energy after counterpoise correction changes only slightly, from 157 to 146 cm^{-1}. In contrast, the basis set enlargement increases both the correlation contribution to the well depth and the counterpoise correction to the correlation effect. These are offsetting changes, and hence, the MP2 interaction energy after counterpoise correction changes only 32 cm^{-1}, from 487 to 519 cm^{-1}. The description of the polarization and dispersion elements of the interaction are surely improved by the addition of diffuse polarization functions, and the 32 cm^{-1} increase in the interaction energy is in line with this description. The increase in counterpoise correction to the correlation energy is attributed to the added diffuse functions helping the correlation description of each partner, partly because of their extensiveness. Diminishment of basis set superposition effects calls for improvement of the core and valence sets of the monomers, though that does not add the flexibility for improving the description of intermolecular polarization. Thus, basis set enlargement in the diffuse regions has largely an orthogonal effect from basis set enlargement in the core and valence regions. For our purposes, it is useful to see that the 40% increase in the number of basis functions in the larger set relative to the cc-pVTZ set affected the counterpoise corrected MP2 interaction energy by only about 6%. We do not expect a significant change from further augmentation with diffuse functions, and we rely on the counterpoise correction for estimating the errors due to lingering deficiencies in the core and valence parts of the basis.

Results of the ACCD calculations, included in Table 1, show the possibility of an overshoot in the correlation effects at the MP2 level. ACCD yields an interaction energy (D_e) diminished by 96 cm^{-1} after counterpoise correction. In the approach to an exact treatment, this difference from the MP2 value could be modified somewhat, including being partly offset by improvements in the basis such as with the 248-function set.

A more complete comparison of the different electronic structure treatments comes from looking at other areas of the surface, not simply a single surface point. The first task to be completed was to find the global equilibrium structure with the different levels of treatment, and Table 2 presents the results obtained, including results for the equilibrium on the counterpoise corrected surfaces. Because the correlation effects and counterpoise corrections do not simply move a surface (or a surface slice) upward or downward but instead slightly change the shape of the surface, there are differences in the optimum separation distances. The counterpoise correction alone lengthens the equilibrium separation distance by 0.09 Å. A further lengthening may arise through more complete treatment of the electron correlation, as found in the ACCD results in Table 2. The sensitivity of the well-depths (stabilities at global equilibrium structures) are less than that found for the single structural point in Table 1. Thus, enlargement of the basis from 176 to 248 functions changes D_e from 490 to 530 cm^{-1}, and using ACCD instead of MP2 for the correlation treatment changes it from 490 to 410 cm^{-1}. Table 3 provides a comparison with prior studies of the acetylene dimer for the equilibrium structure, and there are no unusual differences. The most recent prior ab initio work is that of Karpfen,[17] who has provided comparisons of MP2 results with eight different basis sets.

TABLE 3: Summary of ab Initio Calculations of the Equilibrium Interaction Energy and Separation Distance

calculation	R_{com} (Å)	interaction energy D_e (cm^{-1})
this work (MP2/cc 248 fcns.)	4.358	530
Alberts et al.[13]	4.311	577
Bone and Handy[15]	4.344	551
Hobza et al.[16]	4.493	441
Karpfen (Basis III)[17]	4.31	507

TABLE 4: Symmetry-Constrained Optimum Structures[a] of $(HCCH)_2$ from ab Initio Calculations

	D_{2h} (cross)		C_{2h} (slipped parallel)		
	R_{com} (Å)	interaction energy (cm^{-1})	R_{com} (Å)	θ	interaction energy (cm^{-1})
MP2	3.922	63	4.220	138.1	512
MP2 (SCF/cc)[b]	3.995	64	4.242	138.1	513
MP2/cc	4.096	52	4.288	138.0	439
ACCD/cc	∞	0	4.477	138.3	349

[a] Obtained with the 176-function basis. [b] Counterpoise correction is that of the SCF level treatment only.

Other areas of the surface were considered to obtain a fuller comparison of the different electronic structure treatments. We examined three other structures optimized with symmetry constraints. For the first, a collinear constraint, there was no minimum. The quadrupole−quadrupole repulsion appears sufficient to overcome the dispersion effects and preclude a shallow well, at least at the levels of treatment employed here. Symmetry constrained optimum structures were found for D_{2h} and C_{2h} structures, the former having the acetylenes perpendicular to each other as in a cross and the latter having them parallel but offset or slipped (Figure 1). These surface wells (with constrained symmetry) are features that in part lock in the form of the noncovalent interaction potential between two acetylenes. They were used in constructing surface representations. Table 4 gives the ab initio values obtained for these structures. The interaction energy of the slipped parallel structure is slightly less than the interaction energy at the global minimum (T-shaped). In contrast, the crossed structure is associated with a much smaller dip or well in the surface. At the ACCD level with counterpoise correction, the small dip feature was eliminated by the more complete incorporation of correlation effects, and no minimum was found for the crossed structure. Additional calculations were performed with single substitutions included in the coupled cluster treatment, but their effects were very small, amounting to a less than 0.01 Å change in optimum separation distances and less than 10 cm^{-1} changes in stabilities.

Representations of the Potential Surface

We constructed representations of the potential surfaces with a small number of adjustable parameters and choices of the form of the representation. In all of the cases, the potential for the rigid acetylenes, designating them as A and B, was the following

$$V = E_{\text{electrical}} + \int_i^{\{\text{sites on A}\}} \int_{j>i}^{\{\text{sites on B}\}} \left(\frac{d_i d_j}{r_{ij}^{12}} - \frac{c_i c_j}{r_{ij}^{6}} \right) \quad (1)$$

TABLE 5: Types of Permanent Charge Field Representations Used in the Model Potentials

designation	description
CQ	fixed central quadrupole ($Q_{\|\|} = 1.808$ au)
BD	C−H bond dipoles with adjustable placement along the bond; size fixed to reproduce the molecule's quadrupole used in scheme CQ
DQ	fixed central quadrupole 10% of the size of the quadrupole used in scheme CQ and C−H bond dipoles with adjustable placement and size chosen so that the total molecular quadrupole moment is the same as in scheme CQ

The adjustable parameters were the *c*'s and *d*'s in the 6−12 or Lennard-Jones term of eq 1, and the carbon and hydrogen atoms are the sites. Because of the symmetry of the acetylene monomer, this potential has only four adjustable parameters, a *c*- and *d*-parameter for carbon and for hydrogen centers. The 6−12 term is intended to represent everything apart from the classically evaluated electrical interaction between the monomers, i.e., the energy included in $E_{\text{electrical}}$. The electrical energy was the polarization of each monomer by the permanent charge field of the partner molecule via the dipole and quadrupole polarizabilities, the values of these obtained from prior ab initio calculation,[45] plus the interaction of the permanent moments. The back polarization or mutual polarization contributions were neglected after determining that in the vicinities of the three optimized structures, their contribution is not more than 9 cm^{-1}. This small value is not representative of all weakly bound clusters; for instance, dipolar species will often exhibit greater mutual polarization energetics.

The permanent charge field of acetylene for $E_{\text{electrical}}$ was represented first by two limiting forms labeled CQ and BD, as summarized in Table 5. CQ was simply a central quadrupole, it being the first nonvanishing moment of acetylene. The other limiting description, BD, was that of two C−H bond dipoles. Their magnitude was 0.7638 au, and their positions were ±0.9396 Å from the molecule center. This arrangement yields an overall quadrupole moment identical to the central quadrupole moment used for the first representation. By suitable adjustment of the size of the dipoles, their placement can be essentially anywhere along the molecular axis and yield the same quadrupole. The particular placement we used was from treating the position as an additional adjustable parameter in the first set of searches for *c* and *d* parameters. Sensitivity to small changes in the position was so slight that we did not readjust the position in subsequent searches.

A whole spectrum of representations involving moments through the quadrupole are possible, as well as other representations, and we elected to consider one specific form intermediate between CQ and BD. This form, DQ in Table 5, was chosen to be close to that of the bond dipoles, but included a central quadrupole whose size was set at 10% of the overall molecular quadrupole. The bond dipoles were then dimished in size so that the composite molecular quadrupole matched that of the CQ representation.

For each electrical representation, CQ, BD, and DQ, a series of calculations was performed to search the parameter space of the four adjustable parameters. In each calculation with a model potential, the optimum T-shaped, crossed (D_{2h}), and slipped parallel (C_{2v}) structures were found. The adjustment of the four parameters was to match ab initio values in Table 4 to within certain tolerances. The ab initio results were those from the 176-function basis at the MP2 and ACCD levels, with and without counterpoise correction. Hence, there were 12 model potentials and 12 sets of parameters. The tolerances corresponded to weighting the match for the global equilibrium as the most important and the crossed structure as the least important. After selecting an initial set of tolerances and optimizing the parameters, attempts were made to reduce the largest tolerances. The search stopped when no further improvement could be achieved. The values that remained with large tolerances help identify limitations of the form of the potential. Table 6 gives the values of the 4 parameters for the 12 model potentials, and Table 7 gives the surface features of these 12 potentials that correspond to those obtained by ab initio calculation (Table 4). The disagreement of the model potentials in reproducing Table 4 values is itemized in Table 8. Note that the crossed structure's energy and separation distance are problematic for the CQ electrical representation with the MP2 or MP2/cc ab initio data. This problem is directly related to the attractiveness of the crossed structure at the MP2 level, an attractiveness that is mostly lost at the more complete ACCD level. At the higher correlation level, the CQ representation works about as well as the others.

TABLE 6: Model Potential Parameters (in au)

selection	to match ab initio minima				to match experimental rotational constant[a]	
center	carbon		hydrogen		carbon	hydrogen
parameter	*c*	*d*	*c*	*d*	*d*	*d*
			electrical scheme CQ			
MP2	7.70	3490	0.80	16.0	3703	16.98
ACCD	8.00	3950	0.80	15.0	3812	14.48
MP2/cc	7.80	3800	0.80	20.0	3671	19.32
ACCD/cc	6.40	4050	0.80	13.0	3560	11.43
			electrical scheme BD			
MP2	6.98	2690	0.68	42.0	2932	45.78
ACCD	6.68	3000	0.68	42.0	2943	41.20
MP2/cc	5.98	2800	0.78	50.0	2744	49.00
ACCD/cc	6.10	3350	0.50	36.0	2931	31.50
			electrical scheme DQ			
MP2	6.48	2490	0.78	52.0	2699	56.37
ACCD	5.95	2680	0.65	52.0	2626	50.96
MP2/cc	6.08	2540	0.65	65.0	2474	63.31
ACCD/cc	5.00	3025	0.80	52.0	2632	45.24

[a] The *c* parameters were kept at the values selected from matching minima.

Refinement of the Parameters for the Potential Surfaces via DQMC

Rotational constants were evaluated for each representation of the potential, both the equilibrium value and the ground vibrational state value were obtained from RBDQMC. A comparison with the experimental value of 1856.6 MHz[3] showed that the model potentials were consistently yielding ground vibrational state rotational constants that were larger than the spectroscopic value. This corresponds to the molecules being found, on average, slightly too close in the DQMC simulations with the model potentials. The consistency of this difference suggests that it results from the small, lingering deficiencies in the ab initio surface data. As a means of examining this, we adjusted the nonelectrical parameters in a series of RBDQMC calculations with each representation. The adjustment or refinement was to bring the ground vibrational state rotational constant in line with the spectroscopic value. We found that the smallest change in the parameters needed for this refinement was in changing only the *d* parameters of carbon and hydrogen. These are the parameters used in the repulsive atom−atom R^{-12} term, and a small increase (Table 6), mostly in the carbon parameter, was sufficient to bring about a match with the spectroscopic values for all representations.

TABLE 7: Model Potential Surface Features[a]

ab initio level and el scheme		interaction energies (cm^{-1})			separation distances (Å)			rotational constant (MHz)	
		T	C_{2h}	D_{2h}	T	C_{2h}	D_{2h}	$(B+C)_{eq}/2$	$<B+C>/2$
MP2	CQ	600	500	2	4.284	4.193	5.253	1942	1910
	DQ	606	513	75	4.288	4.221	4.063	1939	1917
	BD	606	520	125	4.286	4.197	3.991	1940	1922
ACCD	CQ	531	439	2	4.381	4.322	5.432	1864	1824
	DQ	508	419	38	4.370	4.326	4.352	1872	1843
	BD	521	431	84	4.373	4.320	4.218	1870	1841
MP2/cc	CQ	524	445	2	4.387	4.290	5.397	1858	1826
	DQ	506	443	49	4.389	4.286	4.220	1857	1837
	BD	504	430	70	4.381	4.292	4.230	1864	1841
ACCD/cc	CQ	414	334	0	4.478	4.444	∞	1790	1739
	DQ	422	330	12	4.472	4.476	4.889	1795	1753
	BD	421	334	44	4.473	4.470	4.566	1793	1751

[a] Model potentials were those in which the *c* and *d* parameters were selected to match ab initio minima.

TABLE 8: Disagreement between ab Initio and Model Values for Potential Surface Features[a]

model		error in interaction energies (cm^{-1})			error in separation distances (Å)		
		T	C_{2h}	D_{2h}	T	C_{2h}	D_{2h}
CQ	MP2	5	12	61	0.002	0.027	1.331
CQ	ACCD	11	8	18	0.007	0.005	0.949
CQ	MP2/cc	34	6	50	0.006	0.002	1.303
CQ	ACCD/cc	4	15		0.006	0.033	
BD	MP2	11	8	62	0.001	0.023	0.069
BD	ACCD	1	13	62	0.001	0.007	0.155
BD	MP2/cc	14	9	18	0.002	0.0004	0.134
BD	ACCD/cc	25	2		0.0	0.002	
DQ	MP2	11	1	12	0.002	0.001	0.141
DQ	ACCD	12	25	16	0.004	0.001	0.021
DQ	MP2/cc	16	4	3	0.008	0.002	0.124
DQ	ACCD/cc	12	19		0.0002	0.0009	

[a] The differences are the absolute differences between values obtained from the model and values obtained from the ab initio level of treatment on which the model was determined.

Certain interesting features are revealed by the values of the parameters in Table 6. First, there is a significant change in the hydrogen parameters with all representations on going from the selection based on ab initio data without counterpoise correction to the corresponding one with counterpoise correction. There is probably a greater basis set superposition effect in the vicinity of the hydrogen centers because of proximity and possibly greater basis deficiency for hydrogen centers than for carbons. Another feature is that the *d* parameter for hydrogen is increased for cases in which the electrical representation uses bond dipoles instead of the central quadrupole. From examining the individual pieces in the interaction energy in eq 1 at equilibrium, we find that the total nonelectrical contribution to the energy changes from 21 cm^{-1} with the CQ scheme to 75 cm^{-1} with the BD scheme. To this extent, the nonelectrical representation can compensate for deficiencies and/or different choices in the electrical part.

The rotational constants at equilibrium with the 12 model potentials after refinement via the DQMC calculations (Table 9) are very similar. Their average differs from the DQMC value (i.e., the experimental value) by 1.6%. This difference is likely a good evaluation of the overall extent of the effect of vibrational averaging on $<B+C>/2$ in the acetylene dimer.

Table 9 gives surface features obtained with the various sets of model potentials. A key result is that upon refinement via RBDQMC, the surface features are very similar, regardless of the level of ab initio treatment used to construct the surface and only slightly more dependent on the electrical representation. Because the DQMC refinement that brings about this similarity was a change in the model *d* parameters, the differences between surfaces using the same electrical representation are mostly in the "size" of the molecules, with the different sizes associated with different deficiencies in the ab initio treatments. However, among electrical representations, there is an important difference in the interaction energy of the crossed form. The use of bond dipoles (BD) instead of a central quadrupole (CQ) yields significantly more attractiveness for the crossed structure. This can be offset, in part, by the parameter selection for the nonelectrical part of the potential, and so, the differences among the potentials with different electrical representations are not striking. The simplest representation, CQ, proves sufficient, particularly by not exaggerating attractiveness in the crossed structure.

Table 10 compares the electrical and nonelectrical interactions with the various models for the T-shaped structure. It should be noted that the nonelectrical term in eq 1 consists of two sums, one attractive and one repulsive. The entire term ends up making a small contribution in the vicinity of the equilibrium, but the individual sums are comparable in size to the electrical interaction energy. The electrical interaction is important but no more dominant in the model than the $1/R^6$ or $1/R^{12}$ nonelectrical terms. The different permanent charge field representations result in only small differences in the net electrical interaction. It is not surprising that these differences are, to a large extent, offset by the nonelectrical terms.

We also note that the T-equilibrium interaction energies from the refined model potentials (Table 9) range from 517 to 552 cm^{-1} for models using the MP2/cc ab initio data and from 501 to 503 cm^{-1} using ACCD/cc ab initio data. A good portion, although not all, of the energy difference of MP2 versus ACCD is erased through the parameter refinement. At the same time, the remaining difference highlights to what extent reproducing the vibrationally averaged rotational constants with a model surface ensures an accurate value for the well depth. Clearly, well-depth variation of around 50 cm^{-1} may go along with little difference in the rotational constants.

Vibrational Effects

The refinement of the model surfaces and their near "convergence" from different starting points makes it meaningful to examine the vibrational averaging effects on the rotational constants and the zero point energy. As already indicated, vibrational averaging affects the value of $(B+C)/2$ for $(HCCH)_2$ by about 1.6%. Table 11 gives the values for the individual constants, *A*, *B*, and *C*. The averaging effects on the components amount to about 2% for *B* and *C* and slightly more than 2% for *A*. The values in Table 11 also show that the final calculated

TABLE 9: Model Potential Surface Features after RBDQMC Parameter Refinement[a]

	interaction energies (cm^{-1})			separation distances (Å)			rotational constant (MHz)	
	T	C_{2h}	D_{2h}	T	C_{2h}	D_{2h}	$(B+C)_{eq}/2$	$<B+C>/2$
electrical scheme CQ								
MP2	548	457	1	4.347	4.264	5.426	1890	1856
ACCD	561	459	4	4.341	4.279	5.230	1895	1857
MP2/cc	552	469	2	4.351	4.249	5.299	1888	1857
ACCD/cc	503	404	0	4.333	4.289	∞	1901	1856
electrical scheme BD								
MP2	542	462	103	4.363	4.284	4.128	1878	1856
ACCD	534	442	88	4.356	4.300	4.187	1883	1856
MP2/cc	517	442	73	4.363	4.271	4.196	1878	1856
ACCD/cc	501	399	61	4.345	4.330	4.312	1892	1856
electrical scheme DQ								
MP2	547	460	61	4.358	4.299	4.207	1882	1856
ACCD	521	430	41	4.352	4.306	4.314	1886	1856
MP2/cc	520	457	52	4.367	4.261	4.179	1875	1856
ACCD/cc	503	395	18	4.344	4.338	4.596	1893	1856

[a] Model d parameters adjusted to match experimental $<B+C>/2$:

TABLE 10: Contributions to the Interaction Energy with the Model Potentials[a]

model:		energetic contributions (cm^{-1})			[eq 1] to the interaction energy	
elect scheme		at a common structure[a]			at the optimum structures[b]	
ab initio basis		electrical	non-electrical		electrical	non-electrical
			original	DQMC-refined		DQMC-refined
CQ	MP2	589	8	−42	573	−25
	ACCD	589	−63	−29	577	−16
	MP2/cc	589	−70	−38	570	−18
	ACCD/cc	589	−202	−87	583	−80
BD	MP2	619	−15	−79	589	−47
	ACCD	619	−101	−86	595	−61
	MP2/cc	619	−99	−103	589	−72
	ACCD/cc	619	−225	−119	593	−92
DQ	MP2	630	−26	−85	603	−56
	ACCD	630	−125	−110	608	−87
	MP2/cc	630	−131	−111	598	−76
	ACCD/cc	630	−237	−128	615	−112

[a] T-shaped structure with $R_{com} = 4.3246$ Å. [b] T-shaped structure with R_{com} at the optimum value for the given model potential.

values are about 10 MHz below experiment[3] for B and about 10 MHz greater for C.

The zero point energy is remarkably uniform, and its average for the 12 model potentials (Table 11) is 130 cm^{-1}. We expect this to be a particularly accurate determination because of its insensitivity to the model potential. Combining this with the large basis ab initio result for D_e (Table 3) yields a value of 400 cm^{-1} for D_0. This happens to match an experimental determination based on infrared intensity measurements.[6] Also, it is within 4 cm^{-1} of an ab initio value, although in that case, D_e was more sizable and offset by a larger zero point energy of 173 cm^{-1}.[13] Of course, our evaluation of the zero point and dissociation energies is for the intermolecular or weak vibrational modes only because HCCH is rigid in the DQMC treatment. Laboratory measurement of D_0 will include the effects of changes in intramolecular modes and will tend to be slightly different.

As a further assessment of the potential and of vibrational features, DQMC calculations were performed for all deuterated forms of the dimer, i.e., those with one, two, three, or four deuterium atoms in place of hydrogens. The potential was the CQ-ACCD/cc model potential, and for these calculations, the number of psips was increased from 8000 to 10 000. The results are given in Table 12. For $(HCCH)_2$, the change in the number of psips affected the value of $<B+C>/2$ by less than 1 MHz. The rotational constants for the deuterated species have been obtained spectroscopically.[7] With one deuterium, one structure was observed,[7] and in our DQMC calculations, those that were biased with different initial starting structures yielded indistinguishable sets of rotational constants and energies. That is, the calculations yielded one state that we associate with the structure observed. It has the single deuterium in the "bonding" position, which would be the position expected to exhibit the most sizable diminishment in zero point energy from deuteration and, thus, the most stable structure. Comparison with the calculated values (Table 12) shows that the $<B+C>/2$ values agree with experimental to 2.7 MHz, or about 0.1%. Furthermore, the small differences for the individual values of A, B, and C are in the same direction and of roughly the same sizes as the differences found for $(HCCH)_2$.

With two deuteriums in the dimer, spectroscopic measurement[7] has found two forms, one with each monomer having a deuterium and the other being the DCCD−HCCH complex. Our DQMC calculations yielded only two distinguishable forms, and their $<B+C>/2$ rotational constants (Table 12) are within 2 MHz of the measured values. With three deuteriums, we obtain rotational constants that match one of the two structures reported.[7] We do not obtain rotational constants consistent with any other structure. Thus, we do not obtain the one designated D1,[7] which has HCCD pointing to the middle of DCCD. However, the DQMC treatment normally selects the vibrational ground state, making excited vibrational states inaccessible. A second conformer of the same molecules, HCCD and DCCD,

TABLE 11: Vibrational Ground State Features

model: elect scheme/ ab initio basis		rotational constants (MHz) A_{eq} $\langle A\rangle$	B_{eq} $\langle B\rangle$	C_{eq} $\langle C\rangle$	interaction energy D_e (cm^{-1}) D_0 (cm^{-1})	zero point energy (cm^{-1})
CQ	MP2	34 895	1941	1839	548	
		33 720	1905	1807	417	131
	ACCD	34 895	1946	1844	561	
		33 820	1906	1808	427	134
	MP2/cc	34 895	1939	1837	552	
		33 660	1906	1807	423	129
	ACCD/cc	34 895	1953	1850	503	
		33 810	1905	1807	372	131
BD	MP2	34 896	1928	1827	542	
		34 140	1904	1807	415	127
	ACCD	34 896	1934	1833	534	
		34 190	1904	1807	405	129
	MP2/cc	34 896	1928	1827	517	
		34 140	1904	1807	391	126
	ACCD/cc	34 896	1943	1840	501	
		34 240	1906	1807	372	126
DQ	MP2	34 896	1937	1836	521	
		34 340	1904	1807	416	131
	ACCD	34 896	1937	1836	521	
		34 370	1891	1796	391	130
	MP2/cc	34 896	1925	1824	520	
		34 320	1904	1808	396	124
	ACCD/cc	34 896	1944	1842	503	
		34 430	1904	1808	370	133
Expt 3		35 188	1914.3	1798.8		

TABLE 12: Vibrational Ground State Features of Deuterated Dimers

cluster[a]	rotational constants (MHz) $\langle A\rangle$	$\langle B\rangle$	$\langle C\rangle$	$<B+C>/2$	interaction energy D_0 (cm^{-1})	zero point energy (cm^{-1})
HCCH−HCCH						
DQMC[b]	33 820	1904	1806	1855	372	131
Expt[3]	35 188	1914.3	1798.8	1856.6		
HCCD−HCCH						
DQMC[b]	33 590	1901	1803	1852	377	126
Expt-A2[7]	35 768	1911.3	1798.0	1854.7		
DCCD−HCCH						
DQMC[b]	32 500	1809	1716	1762	379	124
Expt-B2[7]	35 631	1811.1	1709.1	1760.1		
HCCD−HCCD						
DQMC[b]	28 530	1870	1758	1814	380	123
Expt-C2[7]	30 326	1879.6	1752.0	1815.8		
DCCD−DCCH						
DQMC[b]	24 600	1839	1714	1776	383	120
Expt-D3[7]	26 007	1849.4	1707.9	1778.7		
DCCD−DCCD						
DQMC[b]	24 500	1745	1632	1689	386	117
Expt-E[7]	26 026	1752.0	1624.3	1688.2		

[a] The clusters are specified such that the left monomer points into the middle right monomer and the D or H to the left of the hyphen is the center hydrogen bonding center (Figure 1). The experimental results from ref 7 are given with the identifiers used in that report to the different forms (e.g., A2, D3, etc.). [b] The model potential was that of the CQ representation derived from ACCD/cc ab initio results with DQMC refinement of parameters.

corresponds to an excited state on the whole of the global interaction potential.

The results in Table 12 demonstrate that the reliability of the model potential for ground vibrational state rotational constants shows little sensitivity to substitution of one to four deuterium atoms. That is a good indication of the accuracy of the potential for the regions of the surface sampled in the course of ground vibrational state excursions. The accuracy of the potential in other regions may be worse, but one interesting assessment of that is shown in Figure 2. Model and ab initio calculations were performed to follow the minimum energy path away from the C_{2h} interconversion transition state (a planar structure) as the monomers were twisted out of plane in a concerted fashion that preserves C_2 symmetry (i.e., preserves equivalence of the monomers). The model and ab initio results are not sharply different, and both show a very shallow potential surface slice. There is good agreement in the shaping of the surfaces in this nonequilibrium region. There is, however, a difference in their C_{2h} energies, which serve to reference the energies in Figure 2. The C_{2h} energies are the interconversion barrier heights, and the ab initio ACCD/cc value is 61 cm^{-1} (Tables 2 and 4), whereas the model value after DQMC refinement is 99 cm^{-1} (Table 9, CQ:ACCD/cc). Whether the lingering error in the ab initio calculations or model error is responsible for the difference cannot be determined on the basis of the calculations alone.

Experimental information on the interconversion tunneling frequency is available,[3,4,7] and low-dimensional dynamical

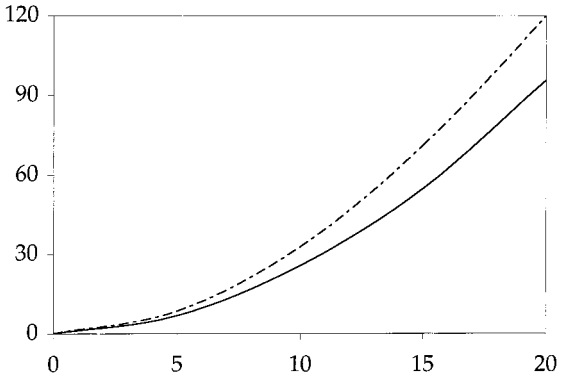

Figure 2. Minimum energy path for the concerted out-of-plane twisting of the acetylenes from the C_{2h} (slipped parallel) transition state structure for the interconversion. The horizontal axis gives the magnitude of the out-of-plane angle for each acetylene, the two molecules being twisted in an opposed sense with C_2 symmetry preserved. The energy in cm^{-1} relative to the optimum C_{2h} structure's energy is the vertical axis. The broken line is that obtained using the model potential of the CQ representation derived from ACCD/cc ab initio results with DQMC refinement of parameters. The solid line is from ab initio MP2/cc calculations with the 176-function basis.

analyses with that information imply barriers of 33.2 cm^{-1} and 35.6 cm^{-1}.[3,7] These are less than our ab initio ACCD/cc value of 61 cm^{-1} and less than other large basis ab initio values such as 59 cm^{-1} and 76 cm^{-1}.[13,11] This may suggest that the true barrier is overvalued even with fairly extensive levels of ab initio treatment, and also, that our model with its still higher barrier is worse. On the other hand, the surface slice in Figure 2 suggests the likelihood for very complicated interconversion dynamics in a way that could make a one-dimensional analysis (to match a measured tunneling frequency) undershoot the true barrier height. Figure 2 shows the variation of the interaction energy with out-of-plane distortion with the acetylenes remaining equivalent in structure. Their equivalence means that each point on the curve in Figure 2 is a structure that is halfway on a path from one T-shape or its interconversion partner T-shape. The potential energy rises quite slowly with the torsional angle, and this means that the interconversion can take place through a range of nonplanar vibrational excursions with about the same energetic ease as through the planar transition state. Hence, a planar treatment of tunneling will necessarily yield less likelihood for interconversion, and in turn, the planar barrier needed to match a measured tunneling splitting will be diminished. We have not sought to concretely establish the barrier height, but the consistency of our calculations, and others done with large basis sets, does not support values for the barrier less than 50 cm^{-1}. With that, the new surface feature revealed in Figure 2 may indicate complexity in the interconversion process that plays a role in the difference.

Conclusions

Ab initio calculations for structures of $(HCCH)_2$ gave energetics and separation distances that were represented by model potentials with three choices for representing acetylene's permanent charge field. The simplest choice, a central quadrupole representation, seemed about as sufficient as the somewhat more complicated distributed forms for this particular dimer. More interesting is that model potentials that were similar in parameter values, surface features, and sizes of energetic elements were obtained for a given electrical representation upon refinement of the repulsive parameters (the *d*'s) so as to match the spectroscopically measured value of $(B + C)/2$ for $(HCCH)_2$. This is a sort of convergence in models that points to the suitability of the form of the functions in the model potential for describing the system in its ground vibrational state. That this form is simple and designed for transferability is important for a larger class of possible applications of the model. It also shows that at the threshold of a large basis set with correlation included, the small lingering errors in ab initio calculations tend to be in the effective sizes of the monomers, a feature we have seen for $Ar-H_2S$ and $Ne-H_2S$.[46] Hence, calculations at simple levels such as MP2 might prove more reliable for similar weakly bound clusters with small, rather easily made adjustments of this sort.

The convergence in the models makes it likely that particularly accurate values for the zero point energy and the zero point dissociation energies have been obtained. These are 130 cm^{-1} and 400 cm^{-1}, respectively. We find the vibrational averaging effect on $(B + C)/2$ to be about 1.6%.

Acknowledgment. This work was supported, in part, by a grant from the Physical Chemistry Program of the National Science Foundation (Grant No. CHE-9714016).

References and Notes

(1) Miller, R. E.; Vohralik, P. F.; Watts, R. O. *J. Chem. Phys.* **1984**, *80*, 5453.
(2) Prichard, D. G.; Nandi, R. N.; Muenter, J. S. *J. Chem. Phys.* **1988**, *89*, 115.
(3) Fraser, G. T.; Suenram, R. D.; Lovas, F. J.; Pine, A. S.; Hougen, J. T.; Lafferty, W. J.; Muenter, J. S. *J. Chem. Phys.* **1988**, *89*, 6028.
(4) Ohshima, Y.; Matsumoto, Y.; Takami, M.; Kuchitsu, K. *Chem. Phys. Lett.* **1988**, *147*, 1.
(5) Bryant, G. W.; Eggers, D. F.; Watts, R. O. *J. Chem. Soc., Faraday* Trans. *2* **1988**, *84*, 1443.
(6) Colussi, A. J.; Sander, S. P.; Friedl, R. R. *Chem. Phys. Lett.* **1991**, *178*, 497.
(7) Matsumura, K.; Lovas, F. J.; Suenram, R. D. *J. Mol. Spectrosc.* **1991**, *150*, 576.
(8) Bhattacharjee, R. L.; Muenter, J. S.; Coudert, L. H. *J. Chem. Phys.* **1992**, *97*, 8850.
(9) Booze, J. A.; Baer, T. *J. Chem. Phys.* **1993**, *98*, 186.
(10) Zhu, Y. F.; Allman, S. L.; Phillips, R. C.; Garrett, W. R.; Chen, C. H., *Chem. Phys. Lett.* **1994**, *224*, 7.
(11) Buck, U.; Ettischer, I.; Schulz, S. *Z. Phys. Chemie* **1995**, *188*, 91.
(12) Aoyama, T.; Matsuoka, O.; Nakagawa, N. *Chem. Phys. Lett.* **1979**, *67*, 508.
(13) Alberts, I. L.; Rowlands, T. W.; Handy, N. C. *J. Chem. Phys.* **1988**, *88*, 3811.
(14) Petrusova, H.; Havlas, Z.; Hobza, P.; Zahradnik, R. *Collect. Czech. Chem. Commun.* **1988**, *53*, 2495.
(15) Bone, R. G. A.; Handy, N. C. *Theor. Chim. Acta* **1990**, *78*, 133.
(16) Hobza, P.; Selzle, H. L.; Schlag, E. W. *Collect. Czech. Chem. Commun.* **1992**, *57*, 1186.
(17) Karpfen, A. *J. Phys. Chem. A* **1999**, *103*, 11 431.
(18) Resende, S. M.; De Almeida, W. B. *Chem. Phys.* **1996**, *206*, 1.
(19) Fraser, G. T. *J. Chem. Phys.* **1989**, *90*, 2097.
(20) Dykstra, C. E. *J. Am. Chem. Soc.* **1990**, *112*, 7540.
(21) Muenter, J. S., *J. Chem. Phys.* **1991**, *94*, 2781.
(22) Suni, I. I.; Klemperer, W. *J. Chem. Phys.* **1993**, *98*, 988.
(23) Assfeld, X.; Almlöf, J. E.; Truhlar, D. G. *Chem. Phys. Lett.* **1995**, *241*, 438.
(24) Dunning, T. H. *J. Chem. Phys.* **1989**, *90*, 1007.
(25) Boys, S. F.; Bernardi, F. *Mol. Phys.* **1970**, *19*, 553.
(26) Chiles, R. A.; Dykstra, C. E. *Chem. Phys. Lett.* **1981**, *80*, 69.
(27) Jankowski, K.; Paldus, J. *Int. J. Quantum Chem.* **1980**, *18*, 1243.
(28) Dykstra, C. E.; Liu, S.-Y.; Daskalakis, M. F.; Lucia, J. P.; Takahashi, M. *Chem. Phys. Lett.* **1987**, *137*, 266.
(29) Dykstra, C. E.; Davidson, E. R. *Int. J. Quantum Chem.*, submitted for publication.
(30) Dykstra, C. E. *J. Am. Chem. Soc.* **1989**, *111*, 6168.
(31) Anderson, J. B. *J. Chem. Phys.* **1975**, *63*, 1499.
(32) Buch, V. *J. Chem. Phys.* **1992**, *97*, 726.
(33) Franken, K. A.; Dykstra, C. E. *J. Chem. Phys.* **1994**, *100*, 2865. Franken, K. A.; Dykstra, C. E. *Chem. Phys. Lett.* **1994**, *200*, 161.
(34) Sandler, P.; Jung, J. O.; Szczesniak, M. M.; Buch, V. *J. Chem. Phys.* **1994**, *101*, 1378.
(35) Gregory, J. K.; Clary, D. C. *Chem. Phys. Lett.* **1994**, *228*, 547.

(36) Gregory, J. K.; Clary, D. C. *J. Chem. Phys.* **1995**, *102*, 7817.
(37) Sandler, P.; Buch, V.; Sadlej, A. J. *J. Chem. Phys.* **1996**, *105*, 10 387.
(38) Niyaz, P.; Bacic, Z.; Moskowitz, J. W.; Schmidt, K. E. *Chem. Phys. Lett.* **1996**, *252*, 23.
(39) Dykstra, C. E. *J. Chem. Phys.* **1998**, *108*, 6619.
(40) Reynolds, P. J. *J. Chem. Phys.* **1990**, *92*, 2118.
(41) Coker, D. F.; Watts, R. O. *J. Phys. Chem.* **1987**, *91*, 2513.
(42) Kalos, M. H. *Phys. Rev. A* **1970**, *2*, 250.
(43) Quack, M.; Suhm, M. A. *J. Chem. Phys.* **1991**, *95*, 28.
(44) Hollenstein, H.; Marquardt, R. R.; Quack, M.; Suhm, M. A. *J. Chem. Phys.* **1994**, *101*, 3588.
(45) Dykstra, C. E.; Liu, S.-Y.; Malik, D. J. *Adv. Chem. Phys.* **1989**, *75*, 37.
(46) de Oliveira, G.; Dykstra, C. E. *J. Chem. Phys.* **1997**, *106*, 5316. de Oliveira, G.; Dykstra, C. E. **1999**, *110*, 289.